

Surface impedance and skin depth for transverse waves in temperature anisotropic unmagnetized plasma

Cite as: Phys. Plasmas **26**, 082116 (2019); <https://doi.org/10.1063/1.5099127>

Submitted: 07 April 2019 . Accepted: 01 August 2019 . Published Online: 20 August 2019

Aman-ur-Rehman , Tajammal H. Khokhar , H. A. Shah , and G. Murtaza 



View Online



Export Citation



CrossMark



ULVAC

Leading the World with Vacuum Technology

- Vacuum Pumps
- Arc Plasma Deposition
- RGAs
- Leak Detectors
- Thermal Analysis
- Ellipsometers



Surface impedance and skin depth for transverse waves in temperature anisotropic unmagnetized plasma

Cite as: Phys. Plasmas **26**, 082116 (2019); doi: 10.1063/1.5099127

Submitted: 7 April 2019 · Accepted: 1 August 2019 ·

Published Online: 20 August 2019



View Online



Export Citation



CrossMark

Aman-ur-Rehman,^{1,2,a)}  Tajammal H. Khokhar,³  H. A. Shah,³  and G. Murtaza³ 

AFFILIATIONS

¹Department of Nuclear Engineering, PIEAS, P.O. Nilore (45650), Islamabad, Pakistan

²Centre for Mathematical Sciences, PIEAS, P.O. Nilore (45650), Islamabad, Pakistan

³Salam Chair, Department of Physics, G. C. University Lahore, Katchery Road, 54000 Lahore, Pakistan

^{a)}Email: amansadiq@gmail.com

ABSTRACT

The anomalous skin depth has been calculated using the surface impedance for the transverse waves in unmagnetized plasma. The effect of temperature anisotropy on the surface impedance and the anomalous skin effect have been studied using the kinetic model for an electromagnetic wave normally impinging on a plasma surface filling the half space $z > 0$. It is noted that the maximum value of the real part of the surface impedance occurs when $\frac{\omega}{\omega_{pe}} = \sqrt{\frac{\pi}{8}} \frac{v_{th}}{c} \sqrt{\frac{T_{\perp}}{T_{\parallel}}}$. The imaginary part, however, is not affected by the temperature anisotropy parameter significantly. It has been found that in the case of anisotropic plasma, the skin depth varies as ω^{-1} in the low frequency regime which is different from isotropic plasma where the skin depth varies as $\omega^{-1/3}$. In the low frequency regime, the skin depth first increases with the temperature anisotropy and then starts decreasing with an increase in the temperature anisotropy parameter η . However, in the large frequency regime, the skin depth is inversely proportional to the temperature anisotropy parameter η . These results have been confirmed by numerically plotting the surface impedance and the skin depth for a wide range of plasma parameters.

Published under license by AIP Publishing. <https://doi.org/10.1063/1.5099127>

I. INTRODUCTION

When the frequency of the electromagnetic (EM) wave is less than plasma frequency, it attenuates upon its interaction with the plasma. This phenomenon is known as the skin depth. The penetration of an electromagnetic (EM) wave inside a plasma depends on numerous parameters such as number density, frequency of the wave, collision frequency of electrons with the background species, thermal speed of the electrons, and the boundary conditions of the plasma reactor in the case of laboratory plasma.^{1–3} As already mentioned, the term skin depth is used to measure the length up to which the field penetrates inside the plasma. Depending on the thermal motion of electrons, the phenomenon of skin depth can be categorized into two kinds. If the electron thermal motion is weak and is not taken into account, the penetration length of EM inside the conducting medium is small and the phenomenon is called the normal skin depth. However, if the thermal motion of the electrons is taken into account, the penetration length of the EM waves inside conducting media is increased. The increase in the skin depth owing to thermal motion of

the electrons is called the phenomenon of anomalous skin effect^{4,5} which is related to the collisionless heating in bounded as well as unbounded plasma (where the plasma dimensions are much larger than the wavelength). In the case of a bounded plasma, the presence of a second boundary influences the penetration of the electromagnetic field inside plasma if the distance between the boundaries, L , satisfies the conditions $L < \lambda$ or $L < \delta$. In the case of discharge plasmas, due to the finite size of the coil producing the radio frequency fields or due to the influence of the metallic boundaries, the electromagnetic fields are spatially inhomogeneous even in the absence of the skin effect. In this case, it becomes necessary to differentiate between the field shielding by the plasma and from the effects of plasma geometry.^{3,6} Some researchers have studied the phenomenon of skin depth in metals,^{7–14} while the others have discussed it theoretically and have performed experimental measurements regarding the skin depth in different types of plasmas.^{15,16}

The skin depth has a wide range of applications in other fields such as laser plasma interaction,¹⁷ material processing,¹⁸ and inductively

coupled plasmas.¹⁹ The penetration of the electromagnetic field inside plasma depends on the plasma frequency which in turn depends on the plasma density through $\omega_{pe} = (\frac{4\pi n_0 e^2}{m_e})^{1/2}$. Here, ω_{pe} is the plasma frequency and n_0 is the plasma density. If the frequency of the penetrating wave $\omega < \omega_{pe}$, then the plasma is called overdense plasma and the penetration of the electromagnetic wave through the plasma is not possible. However, if the frequency of the penetrating wave $\omega > \omega_{pe}$, then the plasma is called underdense plasma and the electromagnetic wave can pass through the plasma. Thus, the frequencies that can pass through the plasma depend on the plasma density. For example, in the case of discharge plasma, the plasma density is of the order of 10^{12} cm^{-3} which corresponds to plasma frequency in the range of about 10 GHz. Now if the frequency of the electromagnetic wave is less than this plasma frequency, the skin effect shall be observed. Similarly, in the case of laser produced plasma, the plasma density is of the order of 10^{15} cm^{-3} which corresponds to plasma frequency which is more than 200 GHz. Now if the frequency of the electromagnetic wave is less than this plasma frequency, the plasma shall be termed as overdense plasma and the phenomenon of skin depth will be observed. Theoretical studies of normal and anomalous skin depth have been performed by well known plasma experts such as Weibel.²⁰ During the propagation of electromagnetic waves in solar winds, the concept of skin depth can be used to understand the mechanism of interaction of solar wind with the Earth's magnetic field, which can be further used for examination of various mechanisms in the magnetosphere.^{21,22}

The particle distribution function has a significant effect on the thermal energy of the electrons and hence on the skin depth inside the plasma. Most of the studies of skin depth have used isotropic distribution functions. However, in certain cases, the velocity distribution function is not isotropic. Anisotropic distribution functions have been observed in experiments when an intense laser interacts with matter, in experiments on plasma processing^{23,24} and during tunnel atom ionization.^{25–28} *In situ* satellite instruments have shown that the terrestrial magnetosphere²⁹ and the solar wind³⁰ contain the electron velocity distribution functions possessing nonthermal properties along with temperature anisotropies. This temperature anisotropy plays a significant role in the fire-hose instability.^{31,32} The distribution functions with temperature anisotropy give rise to new phenomena inside plasma such as Weibel instability.^{33,34} Kaganovich *et al.*^{35,36} and Ferrante *et al.*^{37,38} have discussed the anomalous skin effect in the presence of anisotropic distribution function and compared their results with the isotropic distribution function. However, these studies on the skin depth are qualitative rather than quantitative. Furthermore, they have not derived any expression which relates the skin depth and surface impedance in anisotropically distributed plasma. The real part of surface impedance tells about the power absorption inside plasma, while the imaginary part tells about the phase of the reflected wave. In this work, we have not only derived the formula for the skin depth but also confirmed it by numerically solving the expression for the skin depth. We have also numerically calculated the surface impedance in the presence of temperature anisotropy. A relationship between the skin depth and the surface impedance has been derived. Following is the layout of the paper. In Sec. II, the details of the mathematical model along with the formulas for surface impedance and skin depth have been given. The results and their discussion are given in Sec. III. The summary of the paper is given in Sec. IV.

II. MATHEMATICAL MODEL

In plasmas generated by powerful ultrashort ionizing laser pulses, for example, the kinetic energy of the electrons is very high. Owing to this high electron kinetic energy, the electron-electron and electron-ion collisions are negligible to a large extent.^{34,37–39} This means that above-mentioned plasma can be modeled by using the coupled system of Maxwell and Vlasov equations. The Vlasov equation can be written as

$$\frac{\partial f}{\partial t} + \mathbf{v} \cdot \frac{\partial f}{\partial \mathbf{r}} + \frac{e}{m} \left(\mathbf{E} + \frac{1}{c} \mathbf{v} \times \mathbf{B} \right) \cdot \frac{\partial f}{\partial \mathbf{v}} = 0, \quad (1)$$

and Maxwell's curl equations are given by

$$c \nabla \times \mathbf{E} = - \frac{\partial \mathbf{B}}{\partial t}, \quad (2)$$

$$c \nabla \times \mathbf{B} = 4\pi \mathbf{J} + \frac{\partial \mathbf{E}}{\partial t}. \quad (3)$$

In the above set of equations, f is the velocity distribution function, E is the electric field, B is the magnetic field, J is the current density, c is the speed of light, and e and m are the electron charge and mass, respectively. The Vlasov equation can be linearized by taking $f = f_0 + f_1$, where f_0 is the equilibrium part of the distribution function and f_1 is the perturbed part of the distribution function. The linearized Vlasov equation can be written as

$$\frac{\partial f_1}{\partial t} + \mathbf{v} \cdot \frac{\partial f_1}{\partial \mathbf{x}} + \frac{e}{m} \left(E_1 + \frac{1}{c} \mathbf{v} \times B_1 \right) \cdot \frac{\partial f_0}{\partial \mathbf{v}} + \frac{e}{mc} \mathbf{v} \times \mathbf{B}_0 \cdot \frac{\partial f_1}{\partial \mathbf{v}} = 0.$$

As we have considered the unmagnetized plasma, i.e., $B_0 = 0$, we take in our calculations only the perturbed value of electric and magnetic fields, and the linearized Vlasov equation simplifies to

$$\frac{\partial f_1}{\partial t} + \mathbf{v} \cdot \frac{\partial f_1}{\partial \mathbf{x}} + \frac{e}{m} \left(E_1 + \frac{1}{c} \mathbf{v} \times B_1 \right) \cdot \frac{\partial f_0}{\partial \mathbf{v}} = 0.$$

This system of equations is solved to study the dynamics of the plasma system. Taking the Fourier-Laplace transformation ($\frac{\partial}{\partial t} = -i\omega$; $\frac{\partial}{\partial \mathbf{x}} = i\mathbf{k}$) of the above equations, we get

$$-i\omega f_1 + i\mathbf{v} \cdot \mathbf{k} f_1 + e \left(\mathbf{E}_1 + \frac{1}{c} \mathbf{v} \times \mathbf{B}_1 \right) \cdot \frac{\partial f_0}{\partial \mathbf{v}} = 0.$$

The perturbed part of the distribution function f_1 can be written as

$$f_1 = i \frac{(q_z/m_z)}{\omega - \mathbf{k} \cdot \mathbf{v}} \left(\mathbf{E}_1 \cdot \frac{\partial f_0}{\partial \mathbf{v}} + \frac{1}{c} \mathbf{v} \times \mathbf{B}_1 \cdot \frac{\partial f_0}{\partial \mathbf{v}} \right), \quad (4)$$

and curl Eqs. (2) and (3) can be written in the frequency space as

$$[(\omega^2 - c^2 k^2) \delta_{ij} + c^2 k_i k_j - i4\pi\omega\sigma_{ij}] E_j = 0. \quad (5)$$

Here, σ_{ij} is the conductivity tensor which is expressed using Ohm's law

$$J_i = \sigma_{ij} E_j = q_z \int v_j f_1 d^3 v. \quad (6)$$

Consider the polarization of the wave in which the perturbed magnetic field B_1 , electric field E_1 , and wave vector (k) are taken along

the “x-axis,” “y-axis,” and “z-axis,” respectively. The geometry of the wave is shown in Fig. 1. On simplifying Eqs. (4)–(6), we obtain the dispersion relation for transverse waves in an anisotropic electron plasma,³⁵

$$\frac{c^2 k^2}{\omega^2} = 1 + \frac{4\pi e^2}{m\omega^2} \int dv \left[v_{\perp} \frac{\partial f_0}{\partial v_{\perp}} + \frac{v_{\perp}^2 k}{(\omega - v_{\parallel} k)} \frac{\partial f_0}{\partial v_{\parallel}} \right]. \quad (7)$$

By using the anisotropic Maxwellian distribution and after simplifying, the dispersion relation reduces to

$$\frac{c^2 k^2}{\omega^2} = 1 - \frac{\omega_{pe}^2}{\omega^2} \left[1 - \frac{T_{\perp}}{T_{\parallel}} \{ 1 + \xi Z(\xi) \} \right], \quad (8)$$

where $\xi = \frac{\omega}{kv_{\parallel}}$ and $Z(\xi)$ is the standard plasma dispersion function.

By solving Maxwell’s equation, we obtain

$$\frac{d^2}{dz^2} E_y(z) + \frac{\omega^2}{c^2} E_y(z) = -\frac{4\pi i\omega}{c^2} j_y.$$

The electric field for the semi-infinite geometry is calculated by considering the electric field symmetrically around the plasma, i.e., $E(-z) = E(z)$. The Fourier transform of the electric field is:³⁵

$$E_y(k) = -\frac{2i\omega}{c} B(0) \frac{e^{ikz}}{k^2 - \epsilon_t(\omega, |k|) \frac{\omega^2}{c^2}},$$

where $\epsilon_t(\omega, |k|) = 1 - \frac{\omega_{pe}^2}{\omega^2} \left[1 - \frac{T_{\perp}}{T_{\parallel}} \{ 1 + \xi Z(\xi) \} \right]$.

The spatial profile of the electric field penetrating the plasma can be written by taking the inverse Fourier transform of the above equation

$$E_y(z) = -\frac{i\omega}{\pi c} B(0) \int_{-\infty}^{\infty} \frac{e^{ikz}}{k^2 - \epsilon_t(\omega, |k|) \frac{\omega^2}{c^2}} dk. \quad (9)$$

The surface impedance is defined as⁶

$$\zeta = \frac{4\pi E_y(0)}{c B_x(0)}. \quad (10)$$

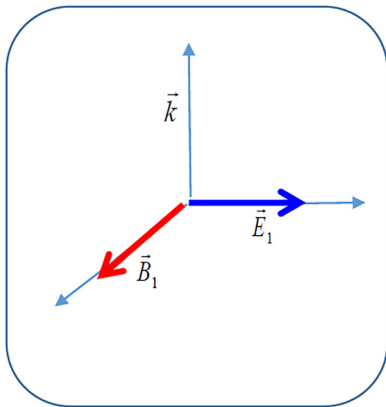


FIG. 1. Geometry of the wave.

Using the above definition, one can write the surface impedance for electromagnetic waves in plasma as follows:

$$\zeta = -\frac{4i\omega}{c^2} \int_{-\infty}^{\infty} \frac{1}{k^2 - \epsilon_t(\omega, |k|) \frac{\omega^2}{c^2}} dk. \quad (11)$$

The surface impedance given by Eq. (11) gives information about the power absorption inside the plasma. The real part gives the absorption coefficient, while the imaginary part tells about the phase of the reflected wave. Kaganovich *et al.* have obtained an analytical expression for the surface impedance which is given by³⁵

$$\zeta = -i \frac{4\pi\omega^2}{\omega_{pe}^2 v_{\perp 1}} + \frac{4\pi\omega/c}{\omega_{pe} \sqrt{\frac{T_{\perp}}{T_{\parallel}} + ic\sqrt{\pi} \frac{\omega}{\sqrt{2}v_{\parallel 1}}}}. \quad (12)$$

In this manuscript, the surface impedance is being used to get information about the field penetration length (i.e., skin depth) inside the plasma. The skin depth can be related to the surface impedance in the following manner. Consider an electromagnetic wave whose electric field is along the y-axis and magnetic field is along the x-axis and is propagating along the z-axis. For this wave, the electric field can be written as

$$E_y(z) = E_y(0)e^{ikz} = E_y(0)e^{i(k_r + ik_i)z}. \quad (13)$$

The magnetic field associated with this wave can be found from Faraday’s law

$$\begin{aligned} \nabla \times \mathbf{E}_y(z) &= -\frac{i\omega \mathbf{B}_x(z)}{c}, \\ \text{or} \\ \frac{E_y(z)}{B_x(z)} &= -\frac{i\omega}{c(k_i - ik_r)}. \end{aligned} \quad (14)$$

Here, we have taken the wave number to be complex and the frequency to be real.^{40,41} The above equation can be used to write an expression for the surface impedance given as

$$\zeta = -\frac{4\pi i\omega}{c^2} \frac{1}{(k_i - ik_r)} = \frac{4\pi\omega}{c^2} \frac{k_r - ik_i}{(k_r^2 + k_i^2)}. \quad (15)$$

Solving this equation for k_i , we can express the skin depth in terms of surface impedance for an electromagnetic wave as

$$\delta = \frac{1}{k_i} = -\frac{c^2}{4\pi\omega} \frac{|\zeta|^2}{\text{Im}[\zeta]}. \quad (16)$$

III. RESULTS AND DISCUSSION

To examine how the temperature anisotropy affects the surface impedance, the integral given in Eq. (11) has been solved numerically to find the real and imaginary parts of the surface impedance. As discussed above, the plasma can be overdense ($\omega < \omega_{pe}$) or underdense ($\omega > \omega_{pe}$) depending on the plasma density and the frequency of the electromagnetic wave. When the plasma density is low, the plasma exhibits overdense behavior for relatively small frequencies, and when the plasma density is high, the plasma exhibits overdense behavior for

relatively large frequencies. So in order to keep discussion valid over a wide range of frequencies and densities, the results have been plotted for normalized frequencies, i.e., as a function of ω/ω_{pe} . All the results presented in this discussion are for overdense plasma where $\omega < \omega_{pe}$. Furthermore, in plasmas generated by a powerful ultrashort ionizing laser pulse, an electron distribution function is created that is anisotropic in the velocity space.^{34–39} In this kind of plasma, the electrons moving in the direction (which is perpendicular to the direction of propagation of the wave) of the ionizing wave electric field extract more energy from the wave as compared to the electrons moving parallel to the direction of propagation of the electromagnetic wave. This results in T_{\perp} (temperature of the electrons moving perpendicular to the direction of propagation of the wave) much more than T_{\parallel} (temperature of the electrons moving parallel to the direction of propagation of the wave). This difference in electron temperature is termed as temperature anisotropy. We have defined a parameter $\eta = \frac{T_{\perp}}{T_{\parallel}}$ to measure temperature anisotropy. For isotropic plasmas, $T_{\perp} = T_{\parallel}$, and hence, $\eta = 1$. The greater the value of η , the more anisotropic the plasma. Figure 2(a) shows that the real part of the surface impedance increases with an increase in the temperature anisotropy for low and intermediate values of ω/ω_{pe} ; however, it becomes very small when ω/ω_{pe} exceeds the value of 0.3. Following Kaganovich *et al.*,³⁵ the real part of the surface impedance can be written as

$$\text{Re}[\zeta] = \frac{4\pi}{c} \frac{\omega}{\omega_{pe}} \left(\frac{\sqrt{\frac{T_{\perp}}{T_{\parallel}}}}{\frac{T_{\perp}}{T_{\parallel}} + \frac{\pi c^2 \omega^2}{8v_{t\parallel}^2 \omega_p^2}} \right). \tag{17}$$

This expression shows that there is a competition between ω/ω_{pe} in the numerator and ω^2/ω_{pe}^2 in the denominator. For small values of the normalized frequency (ω/ω_{pe}), we can neglect ω^2/ω_{pe}^2 in the denominator and the real part of the surface impedance increases with an increase in the value of ω/ω_{pe} . However, when the value of ω/ω_{pe} becomes large depending on the value of temperature anisotropy parameter η , the real part of the surface impedance starts decreasing due to the increase in the value of the second term in the denominator. We also note that the peak of the real part of the surface impedance shifts to higher values of the normalized frequency when the temperature anisotropy parameter η is increased. This dependence of the shift of the peak of $\text{Re}[\zeta]$ on the temperature anisotropy parameter η can be seen by taking the derivative of the above equation with respect to $\frac{\omega}{\omega_{pe}}$ and putting it equal to zero. This analysis shows that the peak of $\text{Re}[\zeta]$ occurs when

$$\frac{\omega}{\omega_{pe}} = \sqrt{\frac{\pi}{8}} \frac{v_{t\parallel}}{c} \sqrt{\frac{T_{\perp}}{T_{\parallel}}} = \sqrt{\frac{\pi}{8}} \frac{v_{t\parallel}}{c} \sqrt{\eta}. \tag{18}$$

This expression shows that the value of the normalized frequency at which peak occurs depends on the square root of the temperature anisotropy parameter. This means that for larger values of the temperature anisotropy parameter, the peak shifts to larger values of ω/ω_{pe} . This behavior can be confirmed by looking at Fig. 2(a). Figure 2(b) shows the plot of the imaginary part of the surface impedance as a function of ω/ω_{pe} . This plot shows that the temperature anisotropy has no effect on the imaginary part of the surface impedance. The magnitude of the imaginary part is very small for small values of the

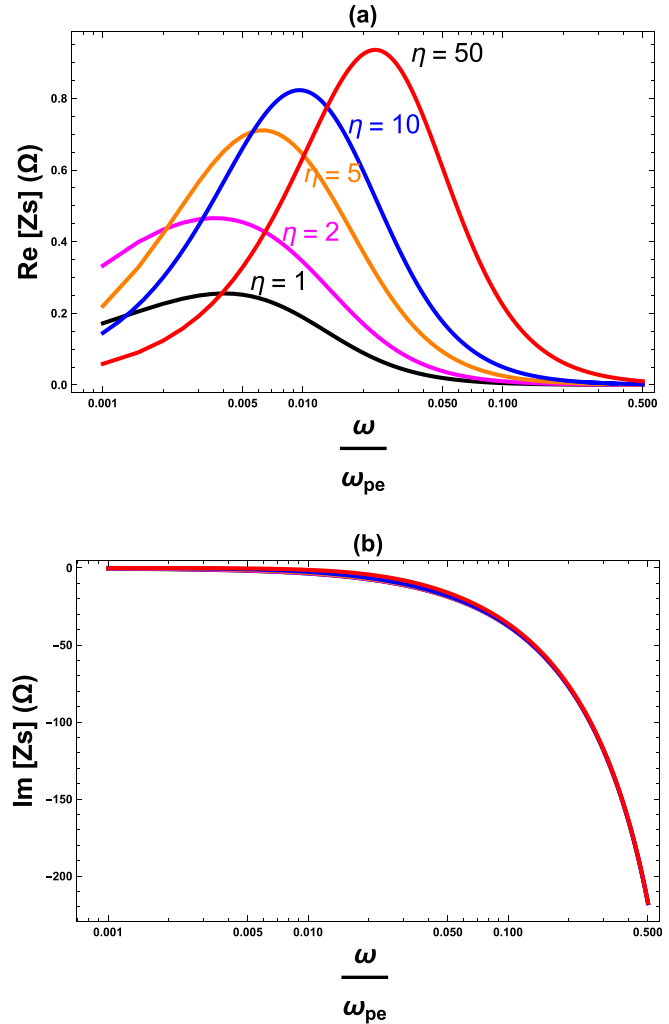


FIG. 2. Real (part a) and imaginary (part b) parts of the surface impedance are plotted for various values of the surface impedance.

normalized frequency; however, it becomes large for larger values of the normalized frequency. Yoon *et al.*⁶ have modeled inductively coupled plasma. In this work, it has been shown that in the case of inductively coupled plasma, the imaginary part of the surface impedance is negative. The part (b) of Fig. 2 shows that the imaginary part of the surface impedance is negative for all values of the frequency, which shows inductive coupling of electromagnetic power to the plasma.

In Fig. 3, we plot the skin depth as a function of ω/ω_{pe} . This figure shows that in the low frequency regime, the skin depth of the anisotropic plasma is larger as compared to the skin depth in isotropic plasma. However, for larger values of the frequency, the skin depth becomes less as compared to the isotropic plasma. When ω/ω_{pe} exceeds 0.1, the skin depth for all the values of the anisotropy parameter converges to the skin depth value for the corresponding isotropic plasma. This dependence of the skin depth on the normalized frequency and the anisotropy parameter can be understood on the basis of the analytical expressions for the skin depth derived from the

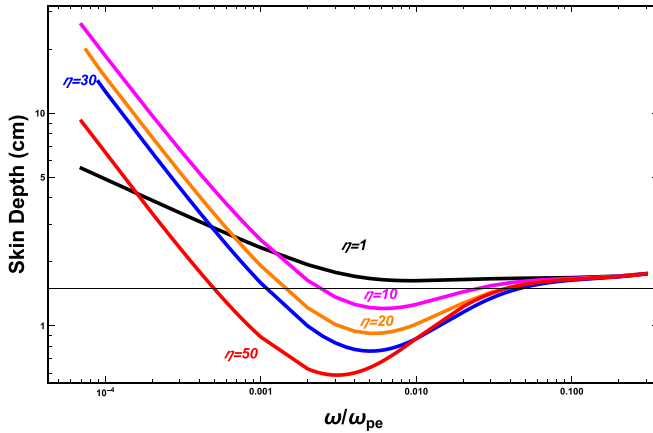


FIG. 3. Skin depth vs normalized frequency for different values of the temperature anisotropy parameter $\eta = \frac{T_{\perp}}{T_{\parallel}}$.

analytical expression for the surface impedance. The anomalous skin depth for isotropic plasma is given by

$$\delta = \left(\frac{c^2 v_{th}}{\omega_{pe}^2 \omega} \right)^{1/3}. \tag{19}$$

This formula shows that for the isotropic plasma, the skin depth varies as $\omega^{-1/3}$ in the low frequency regime. In the case of anisotropic plasma, the surface impedance in the low frequency limit can be written as

$$\zeta = \frac{4\pi}{c} \frac{\omega}{\omega_{pe} \sqrt{\frac{T_{\perp}}{T_{\parallel}} + \frac{ic\sqrt{\pi}\omega}{2\sqrt{2}v_{t\parallel}}}} = 4\pi\omega \left[\frac{\omega_{pe} \sqrt{\frac{T_{\perp}}{T_{\parallel}}} - \frac{ic\sqrt{\pi}\omega}{2\sqrt{2}v_{t\parallel}}}{\omega_{pe}^2 \frac{T_{\perp}}{T_{\parallel}} + \frac{\pi c^2 \omega^2}{8v_{t\parallel}^2}} \right]. \tag{20}$$

The square of the absolute value of ζ and imaginary part of ζ can be written, respectively, as

$$|\zeta|^2 = \frac{16\pi^2 \omega^2}{\omega_{pe}^2 \frac{T_{\perp}}{T_{\parallel}} + \frac{\pi c^2 \omega^2}{8v_{t\parallel}^2}} \tag{21}$$

and

$$\text{Im}|\zeta| = -\frac{4\pi\omega}{c} \left(\frac{c\sqrt{\pi}\omega}{2\sqrt{2}v_{t\parallel}} \right) \frac{1}{\omega_{pe}^2 \frac{T_{\perp}}{T_{\parallel}} + \frac{\pi c^2 \omega^2}{8v_{t\parallel}^2}}. \tag{22}$$

The formula for the skin depth in the low frequency regime can be written as

$$\delta = \frac{1}{k_i} = 2\sqrt{\frac{2}{\pi}} \frac{v_{t\parallel}}{\omega}. \tag{23}$$

This expression shows that for the low frequency regime in the case of anisotropic plasma, the skin depth varies as ω^{-1} . This change

in dependence of the skin depth on the frequency in the presence of anisotropic plasma is responsible for the increase in the skin depth in the low frequency regime. In the large frequency regime, the surface impedance can be written as

$$\zeta = -\frac{i\omega^2 c}{\omega_{pe}^2 v_{t\perp}} + \frac{4\pi\omega^2 \sqrt{\frac{T_{\perp}}{T_{\parallel}}}}{\pi\omega_{pe}^2 v_{t\perp}} = \frac{4\pi\omega^2}{\omega_{pe}^2 v_{t\perp}} \left[\frac{1}{\pi} \sqrt{\frac{T_{\perp}}{T_{\parallel}}} - i \right]. \tag{24}$$

In this case, the square of the absolute value of ζ and imaginary part of ζ can be written, respectively, as

$$|\zeta|^2 = \frac{16\pi^2 \omega^4}{\omega_{pe}^4 v_{t\perp}^2} \left[\frac{1}{\pi^2} \frac{T_{\perp}}{T_{\parallel}} + 1 \right] \tag{25}$$

and

$$\text{Im}|\zeta| = -\frac{4\pi\omega^2}{\omega_{pe}^2 v_{t\perp}}. \tag{26}$$

The expression for the surface impedance in the large frequency regime can be written as

$$\delta = \frac{c^2 \omega}{\omega_{pe}^2 v_{t\perp}} \left[\frac{1}{\pi^2} \left(\frac{T_{\perp}}{T_{\parallel}} \right) + 1 \right]. \tag{27}$$

This expression shows that, in the high frequency regime, the surface impedance is inversely proportional to the temperature anisotropy parameter η . This behavior can be seen in Fig. 3, which shows that the skin depth is small for larger values of temperature anisotropy and the skin depth is large for smaller values of the anisotropy parameter η . This shows that our numerical results are in agreement with the analytical results for the skin depth.

Figures 4 and 5 show the effect of temperature anisotropy on the skin depth in low and high frequency regimes, respectively. Figure 4 shows that in the low frequency regime, the surface impedance first increases with anisotropy, and after reaching a maximum, it starts

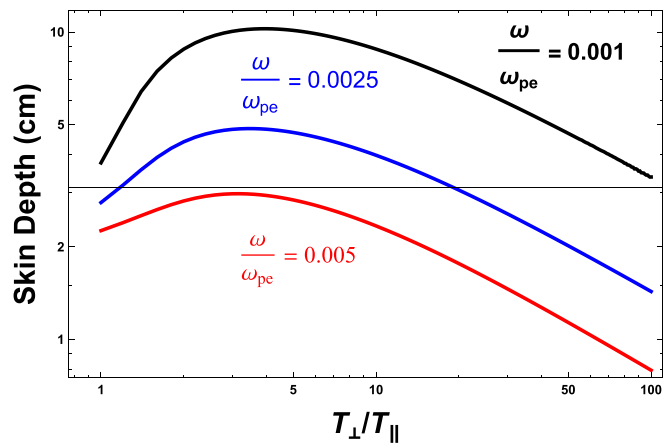


FIG. 4. Skin depth vs temperature anisotropy parameter in the low frequency regime.

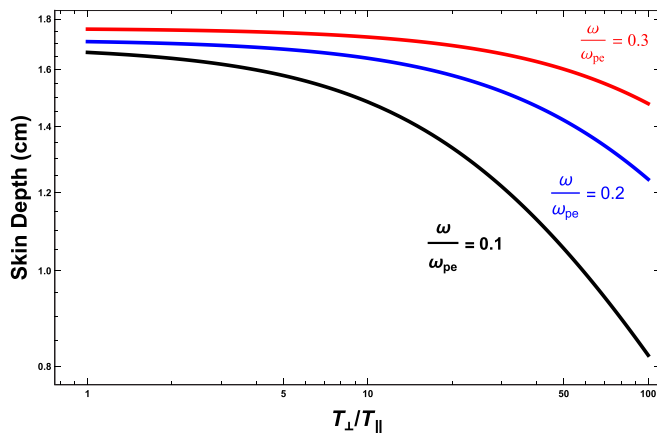


FIG. 5. Skin depth vs temperature anisotropy parameter in the high frequency regime.

decreasing. However, in the large frequency regime shown in Fig. 5, the dependence of the skin depth on temperature is monotonic. This behavior of the dependence of the skin depth on the temperature anisotropy is in agreement with the prediction of Eq. (27). This equation shows that, in the high frequency regime, the skin depth is inversely proportional to the temperature anisotropy.

The skin depth predicted by this model can be confirmed by measuring the electric field profile inside plasma. For this purpose, an experiment can be designed by following Piejak *et al.*^{42,43} In this work, Piejak *et al.* have measured the interaction of the electromagnetic field with the plasma on the basis of the spatial distribution of the time-varying magnetic field. For this purpose, a phase resolved magnetic probe called the dB/dt or B-dot probe is used.^{42,43} The data obtained by a B-dot probe can be used to measure the magnitude of the electric field through Maxwell's equations. Piejak *et al.* have performed experiments in a cylindrical stainless-steel discharge chamber with a Pyrex glass bottom. The B-dot probe consists of three bare wire loops to simultaneously measure B_r and $\frac{dB_z}{dt}$. The B_r loop is one loop turn, while the $\frac{dB_z}{dt}$ loop consists of a single turn in the shape of figure eight. The electric field at position z can be determined by integrating the measured B_r -dot signal along the axial direction.

For an axisymmetric system, the electric field is given by^{42,43} $E_\theta(z) = -10^{-8}i\omega \int B_r(z)dz$, where ω is the driving frequency of the electromagnetic wave, $B_r(z)$ is in Gauss, and the integration along z (in cm) is from the upper wall to the position z inside plasma. The skin depth can be calculated from the electric field profile by measuring the distance of the point where the electric field becomes $1/e$ times the value of the electric field at the surface of the plasma. Piejak *et al.* have shown that for radio frequencies, the electric field decreases very rapidly and the skin depth is of the order of few centimeters,^{42,43} which is in agreement with the prediction of calculations presented in this work.

IV. SUMMARY

The skin depth/spatial damping which is of great interest in both the space and the laboratory plasmas to explain the heating mechanisms has been discussed in this paper. The effect of temperature anisotropy on the surface impedance and the skin depth has been

studied. The results show that the real part of the surface impedance is affected significantly by the temperature anisotropy parameter η , while it has no significant effect on the imaginary part of the surface impedance. Furthermore, it is also found how the skin depth appears in the expression of surface impedance. Numerically calculated values of the real and imaginary parts of surface impedance have been used to calculate the skin depth. The effect of temperature anisotropy on the skin depth has been studied over a large range of frequencies. The results obtained by numerical calculations have been explained by deriving analytical expressions for the skin depth in two limiting cases. It is found that for the anisotropic plasma, in the small frequency regime, the skin depth is inversely proportional to the frequency ω . This dependence of the skin depth on the frequency ω in an anisotropic plasma is different from the dependence of the skin depth on frequency in isotropic plasma. In the case of isotropic plasma, the skin depth varies as $\omega^{-1/3}$. In the large frequency regime, the skin depth increases with the increase in frequency until it approached the skin depth calculated for an isotropic plasma. However, as far as the dependence on the temperature anisotropy parameter is concerned, the skin depth has an inverse relationship with the temperature anisotropy. For low frequencies, the skin depth first increases with the increase in temperature anisotropy and then it starts decreasing with a further increase in the value of η . For high frequencies, the skin depth, however, decreases with an increase in the temperature anisotropy. When the frequency becomes sufficiently large, the skin depth for an anisotropic plasma (for all the values of the temperature anisotropy parameter η) approaches the skin depth value of the corresponding isotropic plasma.

REFERENCES

- V. I. Kolobov and D. J. Economou, *Plasma Sources Sci. Technol.* **6**, R1–R17 (1997).
- A. Rehman and Y. K. Pu, *Phys. Plasmas* **12**, 094503 (2005).
- A. Rehman and Y. K. Pu, *Phys. Plasmas* **13**, 104503 (2006).
- O. V. Polomarov, C. E. Theodosiou, I. D. Kaganovich, D. J. Economou, and B. N. Ramamurthi, *IEEE Trans. Plasma Sci.* **34**, 767 (2006).
- K. Minami and S. Takeda, *Phys. Rev. Lett.* **26**, 614 (1971).
- N. S. Yoon, S. S. Kim, C. S. Chang, and D.-I. Choi, *Phys. Rev. E* **54**, 757 (1996).
- H. London, *Proc. R. Soc. A* **176**, 522 (1940).
- G. E. Smith, *Phys. Rev.* **115**, 1561 (1959).
- K. R. Lyall and J. F. Cochran, *Phys. Rev.* **159**, 517 (1967).
- P. W. Gilbert, *J. Phys. F: Met. Phys.* **12**, 1845 (1982).
- M. I. Kaganov, G. Ya. Lyubarskiy, and A. G. Mitina, *Phys. Rep.* **288**, 291 (1997).
- M. I. Kaganov and P. Contreras, *JETP* **79**, 985 (1994); available at <http://www.jetp.ac.ru/cgi-bin/e/index/e/79/6/p985?a=list>.
- D. C. Mattis and J. Bardeen, *Phys. Rev.* **111**, 412 (1958).
- A. Taguchi, H. Nakane, S. Yamazaki, S. Haseyama, and S. Yoshizawa, *IEEE Trans. Appl. Supercond.* **11**, 3194 (2001).
- A. Macchi, *A Superintense Laser-Plasma Interaction Theory Primer* (Springer, Italy, 2012).
- F. F. Chen, *Phys. Plasmas* **8**, 3008 (2001).
- T. Okumura, *Phys. Res. Int.* **2010**, 164249.
- E. S. Weibel, *Phys. Fluids* **10**, 741 (1967).
- R. G. Storer and C. Meaney, *J. Plasma Phys.* **10**, 349 (1973).
- F. A. Lyman and C. C. Poon, *Phys. Fluids* **14**, 1582 (1971).
- S.-I. Akasofu, *Physics of Magnetospheric Substorms* (D. Reidel, Holland, 1977).
- W. J. Heikkilä, *Earth's Magnetosphere: Formed by the Low-Latitude Boundary Layer* (Elsevier, Oxford, 2011).
- R. C. Davidson, in *Basic Plasma Physics*, edited by A. A. Galeev and R. N. Sudan (North-Holland, Amsterdam, 1983), Vol. 1, p. 519.
- G. Ferrante, M. Zarcone, and S. A. Uryupin, *Plasma Sources Sci. Technol.* **10**, 318 (2001).

- ²⁵P. B. Corkum, N. H. Burnett, and F. Brunel, *Phys. Rev. Lett.* **62**, 1259 (1989).
- ²⁶N. B. Delone and V. P. Krainov, *J. Opt. Soc. Am., B* **8**, 1207 (1991).
- ²⁷W. P. Leemans, C. E. Clayton, W. B. Mori, K. A. Marsh, A. Dyson, and C. Joshi, *Phys. Rev. Lett.* **68**, 321 (1992).
- ²⁸J. C. Kieffer, J. P. Matte, H. Pepin, M. Chaker, Y. Beaudoin, T. W. Johnston, C. Y. Chien, S. Coe, G. Mourou, and J. Dubau, *Phys. Rev. Lett.* **68**, 480 (1992).
- ²⁹S. P. Gary and D. Winske, *J. Geophys. Res.* **105**, 10751, <https://doi.org/10.1029/1999JA000322> (2000).
- ³⁰B. Basu and N. J. Grossbard, *Phys. Plasmas* **18**, 092106 (2011).
- ³¹P. H. Yoon, *Phys. Scr.* **T60**, 127 (1995).
- ³²M. F. Bashir, Z. Iqbal, I. Aslam, and G. Murtaza, *Phys. Plasmas* **17**, 102112 (2010).
- ³³A. Bendib, K. Bendib, and A. Sid, *Phys. Rev. E* **55**, 7522 (1997).
- ³⁴G. Ferrante, M. Zarccone, and S. A. Uryupin, *Phys. Rev. E* **64**, 046408 (2001).
- ³⁵I. Kaganovich, E. Startsev, and G. Shvets, *Phys. Plasmas* **11**, 3328 (2004).
- ³⁶I. D. Kaganovich, O. V. Polomarov, and C. E. Theodosiou, *IEEE Trans. Plasma Sci.* **34**, 696 (2006).
- ³⁷G. Ferrante, M. Zarccone, and S. A. Uryupin, *Eur. Phys. J. D* **19**(3), 349 (2002).
- ³⁸G. Ferrante, M. Zarccone, and S. A. Uryupin, *Phys. Rev. Lett.* **91**, 085005 (2003).
- ³⁹G. Ferrante, M. Zarccone, and S. A. Uryupin, *Eur. Phys. J. D* **22**, 109 (2003).
- ⁴⁰T. H. Khokhar, M. F. Bashir, P. H. Yoon, R. A. López, and G. Murtaza, *Phys. Plasmas* **25**, 084501 (2018).
- ⁴¹T. H. Khokhar, P. H. Yoon, R. A. López, and G. Murtaza, *Phys. Plasmas* **25**, 082114 (2018).
- ⁴²R. B. Piejak, V. A. Godyak, and B. M. Alexandrovich, *J. Appl. Phys.* **81**, 3416 (1997).
- ⁴³V. A. Godyak and R. B. Piejak, *J. Appl. Phys.* **82**, 5944 (1997).